JACS
JOURNAL OF THE AMERICAN CHEMICAL SOCIETY
Cite This: J. Am. Chem. Soc. 2018, 140, 5330−5333
Communication
pubs.acs.org/JACS

3D Anionic Silicate Covalent Organic Framework with srs Topology

Oussama Yahiaoui,[†] Andrew N. Fitch,[‡] Frank Hoffmann,[§] Michael Fröba,[§] Arne Thomas,*[,†] and Jérôme Roeser*[,†]

[†]Department of Chemistry, Technische Universität Berlin, BA2, Hardenbergstraße 40, 10623 Berlin, Germany
[‡]European Synchrotron Radiation Facility, CS40220, 38043 Grenoble Cedex 9, France
[§]Institute of Inorganic and Applied Chemistry, University of Hamburg, Martin-Luther-King Platz 6, 20146 Hamburg, Germany

Supporting Information

ABSTRACT: The synthesis of 3D covalent organic frameworks (COFs) adopting novel topologies is challenging, and so far 3D COFs have only been reported for nets based on building blocks with tetrahedral geometry. We demonstrate the targeted synthesis of an anionic 3D COF crystallizing in a three-coordinated **srs** net by exploiting a recently developed linkage for the formation of anionic silicate COFs based on hypercoordinate silicon nodes. The framework, named SiCOF-5, was synthesized by reticulating dianionic hexacoordinate $[SiO_6]^{2-}$ nodes with triangular triphenylene building blocks and adopts a two-fold interpenetrated **srs-c** net with an overall composition of $Na_2[Si(C_{18}H_6O_6)]$ (where $C_{18}H_6O_6$ is triphenylene-2,3,6,7,10,11-hexakis(olate)). A key requirement for the crystallization of SiCOF-5 was the careful control over the nucleation and growth rate by gradual generation of the silicon source during the course of the reaction.

Covalent organic frameworks (COFs) are porous extended crystalline frameworks solely composed of organic building blocks linked through strong covalent bonds.[1] COFs are synthesized by design following the principles of reticular chemistry,[2] which allows a precise control over their pore structure and the arrangement of chemical functionalities according to the connectivity and the geometry of the rigid building blocks used for their construction. COFs have thus emerged as an important class of materials and hold promise for improved performance in applications such as gas storage and separation,[3] heterogeneous catalysis,[4] proton and ion conduction,[5] and optoelectronics.[6] As with any class of materials, COFs would benefit from increased compositional and structural complexity, and a major challenge in the development of this class of material lies in the expansion of linkages (bonds formed to reticulate the building blocks), composition, and topologies (underlying nets describing such frameworks). In terms of structure, the field is dominated by 2D COFs, and most of the COFs reported consist of extended 2D layers stacking up in the third direction to form an overall 3D framework with unidirectional pore channels. Most topologies of 2D frameworks with minimal transitivity (the most symmetric nets) have been reported,[1a,7] and materials with a high degree of compositional and structural complexity, such as multi-component or multi-pore COFs, have been achieved.[8] 3D COFs have been developed to a lesser extent, especially in terms of accessible topologies, whereby only five distinct 3D topologies are currently described for COFs,[1b,9] a number that is considerably smaller compared to the amount of different topologies reported for the two other classes of porous crystalline framework materials (metal−organic frameworks (MOF) and zeolites).[10] In terms of composition, various functionalities have been successfully introduced pre- and postsynthetically in COF backbones by exploiting an extensive library of tailor-made building blocks.[11] Notably, focus has recently turned to the introduction of ionic functionalities in the skeleton of COFs. Initially reported for amorphous microporous polymer networks,[12] the incorporation of permanent charges into porous organic frameworks holds promise for the generation of COFs with improved performance as solid electrolytes, heterogeneous catalysts, sensors and in gas storage applications.[9c,13] Here we report the synthesis of SiCOF-5, a 3D anionic COF crystallizing in the three-coordinated (3-c), two-fold interpenetrated **srs-c** net, one of the five regular nets (nets with transitivity 1111) described in the Reticular Chemistry Structure Resource (RCSR) but never reported for COFs.[14] Our strategy exploits a new linkage recently developed in our laboratory by implementing reversible Si−O chemistry for the reticulation of ditopic catecholate linkers around dianionic hexacoordinate silicon vertices to form extended 2D anionic frameworks (2D SiCOFs).[15] In a way similar to that for reported transition metal catecholate frameworks,[16] 3D frameworks with **srs** topology should form when such octahedral silicate centers are linked with tritopic catecholate building blocks (Scheme 1).

Despite multiple attempts, no crystalline frameworks could be obtained by condensation of 2,3,6,7,10,11-hexahydroxytriphenylene (HHTP) and silica gel or tetramethoxysilane (TMOS) as silicon source. Developing a new linkage is challenging, and although for other COF linkages the initially reported reaction conditions proved to be appropriate for the crystallization of an extended number of monomer combinations, adjustments of the reaction conditions were sometimes required to successfully obtain the targeted crystalline product.[17] One key consideration is to carefully control the rate of reaction and find the specific conditions appropriate for crystal nucleation and growth. For MOFs this was initially achieved by controlling the rate of deprotonation of carboxylic acids. Approaches used for that purpose include diluting the base in the reaction media or in situ generation of the base by decomposition of *N*,*N*-dimethylformamide.[18] For COFs, control over reaction rate was

Received: February 12, 2018
Published: April 4, 2018

ACS Publications © 2018 American Chemical Society

DOI: 10.1021/jacs.8b01774
J. Am. Chem. Soc. 2018, 140, 5330−5333

Scheme 1. Linking Octahedral Silicate Centers with Tritopic Catecholate Building Blocks[a]

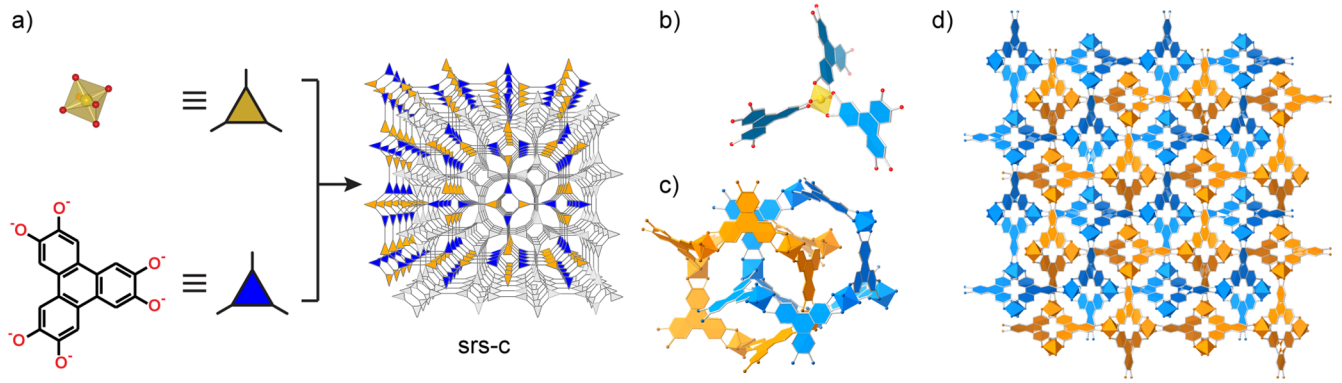

[a](a) The underlying net of SiCOF-5 is composed of triangular $Si(O_2)_3$ dianions (yellow triangles) linked via triangular deprotonated HHTP building blocks (blue triangles). The resulting augmented net is a doubly interpenetrated 3-c **srs-c** net. Schematic representations are presented of a guest-free SiCOF-5 framework (d) composed of SiO_6 and triphenylene nodes (b) extending in two interpenetrated nets (c). Extra-framework cations are omitted for clarity.

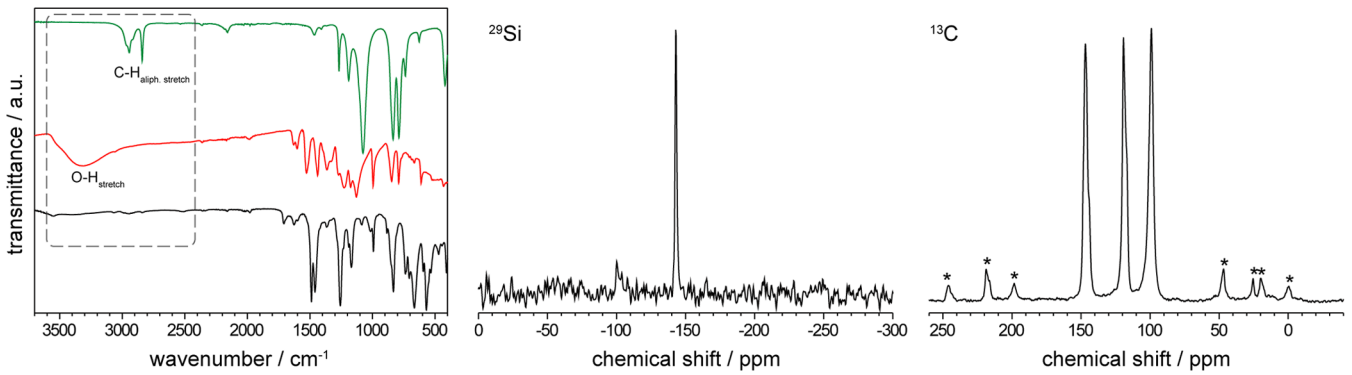

Figure 1. (Left) FTIR spectra of MTMS (green curve), HHTP (red curve), and as-synthesized SiCOF-5 (black curve). (Middle) ^{29}Si and (right) ^{13}C CP-MAS NMR spectra of SiCOF-5; asterisks denote spinning sideband signals and the presence of residual acetone (27 ppm) and methanol (47 ppm) solvent molecules.

initially theorized to occur by controlling the solubility of the linkers and the amount of water in the closed reaction system. Recently, control of the nucleation and growth of interwoven imine COFs was demonstrated by gradual in situ generation of amines.[19] In this context, we hypothesized that controlling the amount of in situ generated silicon source might favor the crystallization of SiCOFs. This challenge can be addressed by gradually generating TMOS in the reaction media by disproportionation of organosilanes in the presence of strong nucleophilic agents. Interestingly, the formation of TMOS from organosilanes was reported to occur in the presence of alkali metal methoxide bases under reaction conditions similar to those used for the formation of the 2D SiCOFs.[20] We thus investigated the crystallization of SiCOF-5 starting with methyltrimethoxysilane (MTMS) as silicon precursor. An excess of MTMS was used in order to account for its possible overall disproportionation into TMOS and tetramethylsilane (Supporting Information (SI), section S2). We found that reacting HHTP with 1.5 equiv of MTMS solvothermally in methanol at 180 °C for 4 days in the presence of sodium methoxide leads to the formation of the polycrystalline SiCOF-5.

The structural integrity of the framework was initially assessed by Fourier transform infrared (FTIR) spectroscopy (Figure 1a). The FTIR spectrum of SiCOF-5 contained strongly attenuated O−H stretching vibrations (3100−3600 cm^{-1}) indicative of successful condensation of the reactants. Furthermore, the absence of aliphatic C−H stretching bands (2800−3000 cm^{-1}) confirmed the full condensation and gave a first indication of Si−C bond cleavage in the starting MTMS during the course of the reaction. The formation of an extended framework composed of hexacoordinate dianionic SiO_6 centers was unambiguously determined by cross-polarization magic-angle spinning nuclear magnetic resonance (CP-MAS NMR). One single signal with a chemical shift of −143 ppm could be observed in the ^{29}Si CP-MAS NMR spectrum of SiCOF-5, indicative of the presence of solely SiO_6 vertices within the entire framework (Figure 1b).[15,21] ^{13}C CP-MAS NMR confirmed the cleavage of the Si−C bond, as no signal attributable to this carbon could be identified, whereas the expected signals for the aromatic carbons of HHTP were observed (Figure 1c). The presence of sodium cations compensating the negatively charged vertices was confirmed by the presence of one single signal at −34 ppm in the ^{23}Na MAS NMR spectrum (SI, Figure S1). The stoichiometric amount of Na was confirmed by inductively coupled plasma atomic emission spectroscopy (ICP-AES) and energy-dispersive X-ray (EDX) analyses, from which the expected 2/1 (Na/Si) ratio was observed (SI, Figure S4 and section S2). Further investigations by compositional and ICP analyses indicated a strong deviation from the theoretical composition of a guest-free framework. The presence of additional signals that can be assigned to acetone (27 ppm) and methanol (47 ppm) solvent molecules in the ^{13}C CP-MAS NMR spectrum and careful evaluation of the acid-digested

DOI: 10.1021/jacs.8b01774
J. Am. Chem. Soc. 2018, 140, 5330−5333

samples by ^{1}H NMR indicated the presence of an integrated ratio of 2.6 molecules of methanol and an additional 0.4 molecule of acetone per repeating unit (SI, Figure S2). Thus, it can be assumed that most of the extra-framework Na counterions are coordinated by solvent molecules and are not present as "naked ions". An overall good agreement was found between the chemical formulation of the frameworks and the experimentally obtained compositional analyses (SI, section S2).

For structural elucidation, high-resolution PXRD diffraction patterns were collected using a synchrotron radiation source (λ = 0.399911(2) Å, ID22 beamline, ESRF). Sharp reflections that could not be attributed to the starting monomer indicated the formation of a framework with a high level of crystallinity (Figure 2, SI, Figure S6). The PXRD pattern could be indexed

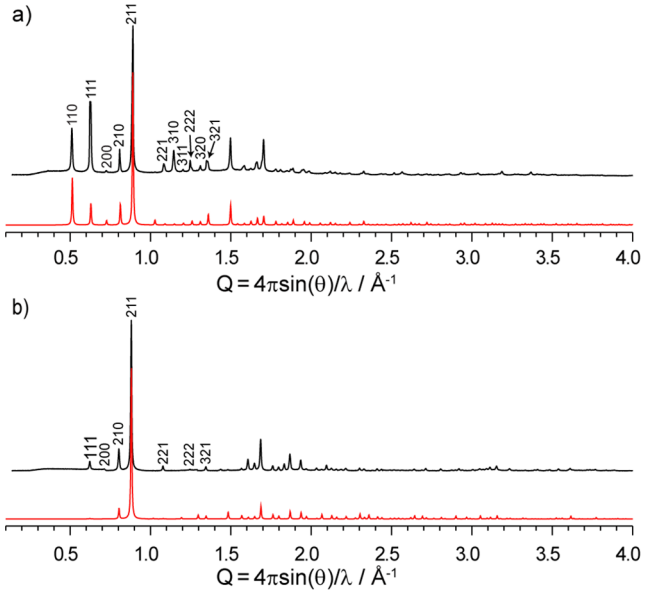

Figure 2. Simulated (red curves) and high-resolution experimental (black curves) PXRD patterns of the (a) as-synthesized and (b) air-exposed SiCOF-5.

compatible with a unit cell of pseudo-cubic metric (a = 17.2703 Å) in the space group $R\bar{3}$ (No. 148), belonging to the trigonal crystal system. The underlying net, and notably the degree of interpenetration of the framework, was initially evaluated by generating the guest-free chiral **srs** net and the overall racemic **srs-c** net composed of two interpenetrated **srs** nets with opposite chirality (SI, section S5). Comparison of the simulated and experimental PXRD patterns indicated an overall better match with the two-fold interpenetrated model (SI, Figure S10). The major discrepancies in terms of reflection intensities between the simulated and the experimental patterns, especially in the small Q region, can be accounted for by the influence of the guests not included in these initial models. Thus, based on the indication obtained from compositional analyses, additional electron density was then accommodated within the computational models by inserting a stoichiometric amount of sodium counterions and the determined amount of additional solvent molecules. A good agreement was found in terms of reflection intensities between the simulated patterns of the refined model and the experimental pattern, thus validating the crystallization of the framework in a **srs-c** net (Figure 2a). Note that the remaining differences in terms of intensities between the simulated and the experimental pattern arise from the difficulty in properly accounting for the position of disordered Na^+ ions and solvent molecules in an ideal single-crystal simulated model. The morphology of SiCOF-5 nanocrystals was investigated by scanning electron microscopy analysis and revealed the formation of homogeneous cubic crystallites (SI, Figure S5). The architectural stability and permanent porosity of SiCOF-5 were investigated by thermogravimetric analysis (TGA) and nitrogen sorption experiments at 77 K. The apparent surface area (S_{BET}) was calculated to be 370 $m^2 \cdot g^{-1}$ from the Brunauer–Emmett–Teller (BET) model (SI, Figure S12). This value is in the same range as the S_{BET} measured for the **srs-c** metal–catecholate framework Ti-CAT-5.[16] The TGA curve of SiCOF-5 displayed a gradual weight loss after 100 °C that could be attributed to the delayed removal of the strongly coordinated solvent molecules. Thus, the theoretical full thermal activation is difficult to achieve, as it occurs only at high temperatures (500 °C) at which framework decomposition occurs simultaneously (Figure S13). The air stability of the framework was investigated by PXRD analysis and revealed that a phase change occurred after contact with air (SI, Figure S7). The pattern of the air-exposed framework could be indexed according to a cubic unit cell ($Pa\bar{3}$, No. 205) with slightly larger lattice parameters (a = 17.449 Å) compared to the as-synthesized framework. A procedure similar to that used for the as-synthesized framework was used to carefully evaluate the chemical composition of the air-exposed framework. Notably, ^{1}H NMR (SI, Figure S3) spectroscopy, FTIR (SI, Figure S13), and compositional analyses (SI, section S2) indicated that the organic solvent molecules are no longer present after air-exposure and that a high water uptake occured upon exposure to air humidity. The computational models were refined by taking into account the determined electron density, leading to a satisfying model according to the overall good agreement between the simulated and experimental PXRD patterns (Figure 2b, SI, Figure S11). The chemical stability of the frameworks was evaluated by immersing the framework in different solvents for 1 day, whereby the frameworks were recovered quantitatively, and no sign of loss of crystallinity was observed by PXRD analyses, indicating that the crystallinity was retained (SI, Figure S15).

In summary, we report the design and synthesis of an anionic 3D COF crystallizing in the **srs** topology. This work demonstrates the importance and the challenge of developing new linkages for the elaboration of anionic COFs. Indeed, the implementation of reversible Si–O chemistry to reticulate COFs around hypercoordinate silicon linkages allowed us to expand the scope of topologies described for COFs, as the three-coordinated **srs** topology was not previously described for 3D COFs and so far the use of tetrahedral building blocks was mandatory to obtain such 3D structures. Moreover, the reaction conditions had to be carefully adapted in order to synthesize the targeted structure, and a strategy to gradually release active silicon source had to be adopted in order to control the rate of nucleation and growth of the framework.

■ ASSOCIATED CONTENT

Supporting Information

The Supporting Information is available free of charge on the ACS Publications website at DOI: 10.1021/jacs.8b01774.

Full synthetic procedures and characterization data, PXRD analyses, and structure models details (PDF)

Crystal structures of as-synthesized Si-COF-5 (CIF)

Crystal structures of air-exposed Si-COF-5 (CIF)

DOI: 10.1021/jacs.8b01774
J. Am. Chem. Soc. 2018, 140, 5330–5333

AUTHOR INFORMATION

Corresponding Authors

*arne.thomas@tu-berlin.de

*jerome.roeser@tu-berlin.de

ORCID

Arne Thomas: 0000-0002-2130-4930

Notes

The authors declare no competing financial interest.

ACKNOWLEDGMENTS

This work was financially supported by the Cluster of Excellence Unifying Concepts in Catalysis (UniCat) funded by the German Science Foundation (DFG).

REFERENCES

(1) (a) Côté, A. P.; Benin, A. I.; Ockwig, N. W.; O'Keeffe, M.; Matzger, A. J.; Yaghi, O. M. *Science* **2005**, *310*, 1166. (b) El-Kaderi, H. M.; Hunt, J. R.; Mendoza-Cortés, J. L.; Côté, A. P.; Taylor, R. E.; O'Keeffe, M.; Yaghi, O. M. *Science* **2007**, *316*, 268. (c) Kuhn, P.; Antonietti, M.; Thomas, A. *Angew. Chem., Int. Ed.* **2008**, *47*, 3450. (d) Feng, X.; Ding, X.; Jiang, D. *Chem. Soc. Rev.* **2012**, *41*, 6010. (e) Kandambeth, S.; Mallick, A.; Lukose, B.; Mane, M. V.; Heine, T.; Banerjee, R. *J. Am. Chem. Soc.* **2012**, *134*, 19524. (f) Ascherl, L.; Sick, T.; Margraf, J. T.; Lapidus, S. H.; Calik, M.; Hettstedt, C.; Karaghiosoff, K.; Döblinger, M.; Clark, T.; Chapman, K. W.; Auras, F.; Bein, T. *Nat. Chem.* **2016**, *8*, 310. (g) Auras, F.; Ascherl, L.; Hakimioun, A. H.; Margraf, J. T.; Hanusch, F. C.; Reuter, S.; Bessinger, D.; Döblinger, M.; Hettstedt, C.; Karaghiosoff, K.; Herbert, S.; Knochel, P.; Clark, T.; Bein, T. *J. Am. Chem. Soc.* **2016**, *138*, 16703. (h) Diercks, C. S.; Yaghi, O. M. *Science* **2017**, *355*, eaal1585.

(2) Yaghi, O. M.; O'Keeffe, M.; Ockwig, N. W.; Chae, H. K.; Eddaoudi, M.; Kim, J. *Nature* **2003**, *423*, 705.

(3) (a) Furukawa, H.; Yaghi, O. M. *J. Am. Chem. Soc.* **2009**, *131*, 8875. (b) Doonan, C. J.; Tranchemontagne, D. J.; Glover, T. G.; Hunt, J. R.; Yaghi, O. M. *Nat. Chem.* **2010**, *2*, 235. (c) Rabbani, M. G.; Sekizkardes, A. K.; Kahveci, Z.; Reich, T. E.; Ding, R.; El-Kaderi, H. M. *Chem. - Eur. J.* **2013**, *19*, 3324. (d) Huang, N.; Chen, X.; Krishna, R.; Jiang, D. *Angew. Chem., Int. Ed.* **2015**, *54*, 2986.

(4) (a) Ding, S.-Y.; Gao, J.; Wang, Q.; Zhang, Y.; Song, W.-G.; Su, C.-Y.; Wang, W. *J. Am. Chem. Soc.* **2011**, *133*, 19816. (b) Stegbauer, L.; Schwinghammer, K.; Lotsch, B. V. *Chem. Sci.* **2014**, *5*, 2789. (c) Lin, S.; Diercks, C. S.; Zhang, Y.-B.; Kornienko, N.; Nichols, E. M.; Zhao, Y.; Paris, A. R.; Kim, D.; Yang, P.; Yaghi, O. M.; Chang, C. J. *Science* **2015**, *349*, 1208. (d) Xu, H.; Gao, J.; Jiang, D. L. *Nat. Chem.* **2015**, *7*, 905. (e) Vyas, V. S.; Haase, F.; Stegbauer, L.; Savasci, G.; Podjaski, F.; Ochsenfeld, C.; Lotsch, B. V. *Nat. Commun.* **2015**, *6*, 8508. (f) Pachfule, P.; Acharjya, A.; Roeser, J.; Langenhahn, T.; Schwarze, M.; Schomäcker, R.; Thomas, A.; Schmidt, J. *J. Am. Chem. Soc.* **2018**, *140*, 1423.

(5) (a) Chandra, S.; Kundu, T.; Kandambeth, S.; Babarao, R.; Marathe, Y.; Kunjir, S. M.; Banerjee, R. *J. Am. Chem. Soc.* **2014**, *136*, 6570. (b) Vazquez-Molina, D. A.; Mohammad-Pour, G. S.; Lee, C.; Logan, M. W.; Duan, X.; Harper, J. K.; Uribe-Romo, F. J. *J. Am. Chem. Soc.* **2016**, *138*, 9767. (c) Xu, H.; Tao, S.; Jiang, D. *Nat. Mater.* **2016**, *15*, 722.

(6) (a) Wan, S.; Gándara, F.; Asano, A.; Furukawa, H.; Saeki, A.; Dey, S. K.; Liao, L.; Ambrogio, M. W.; Botros, Y. Y.; Duan, X.; Seki, S.; Stoddart, J. F.; Yaghi, O. M. *Chem. Mater.* **2011**, *23*, 4094. (b) DeBlase, C. R.; Silberstein, K. E.; Truong, T.-T.; Abruña, H. D.; Dichtel, W. R. *J. Am. Chem. Soc.* **2013**, *135*, 16821. (c) Mulzer, C. R.; Shen, L.; Bisbey, R. P.; McKone, J. R.; Zhang, N.; Abruña, H. D.; Dichtel, W. R. *ACS Cent. Sci.* **2016**, *2*, 667.

(7) (a) Spitler, E. L.; Dichtel, W. R. *Nat. Chem.* **2010**, *2*, 672. (b) Zhou, T.-Y.; Xu, S.-Q.; Wen, Q.; Pang, Z.-F.; Zhao, X. *J. Am. Chem. Soc.* **2014**, *136*, 15885. (c) Dalapati, S.; Addicoat, M.; Jin, S.; Sakurai, T.; Gao, J.; Xu, H.; Irle, S.; Seki, S.; Jiang, D. *Nat. Commun.* **2015**, *6*, 7786.

(8) (a) Zhu, Y.; Wan, S.; Jin, Y.; Zhang, W. *J. Am. Chem. Soc.* **2015**, *137*, 13772. (b) Huang, N.; Zhai, L.; Coupry, D. E.; Addicoat, M. A.; Okushita, K.; Nishimura, K.; Heine, T.; Jiang, D. *Nat. Commun.* **2016**, *7*, 12325. (c) Cai, S.-L.; Zhang, K.; Tan, J.-B.; Wang, S.; Zheng, S.-R.; Fan, J.; Yu, Y.; Zhang, W.-G.; Liu, Y. *ACS Macro Lett.* **2016**, *5*, 1348. (d) Pang, Z.-F.; Xu, S.-Q.; Zhou, T.-Y.; Liang, R.-R.; Zhan, T.-G.; Zhao, X. *J. Am. Chem. Soc.* **2016**, *138*, 4710. (e) Qian, C.; Qi, Q.-Y.; Jiang, G.-F.; Cui, F.-Z.; Tian, Y.; Zhao, X. *J. Am. Chem. Soc.* **2017**, *139*, 6736.

(9) (a) Uribe-Romo, F. J.; Hunt, J. R.; Furukawa, H.; Klöck, C.; O'Keeffe, M.; Yaghi, O. M. *J. Am. Chem. Soc.* **2009**, *131*, 4570. (b) Lin, G.; Ding, H.; Yuan, D.; Wang, B.; Wang, C. *J. Am. Chem. Soc.* **2016**, *138*, 3302. (c) Zhang, Y.; Duan, J.; Ma, D.; Li, P.; Li, S.; Li, H.; Zhou, J.; Ma, X.; Feng, X.; Wang, B. *Angew. Chem., Int. Ed.* **2017**, *56*, 16313.

(10) (a) Furukawa, H.; Cordova, K. E.; O'Keeffe, M.; Yaghi, O. M. *Science* **2013**, *341*, 1230444. (b) Li, M.; Li, D.; O'Keeffe, M.; Yaghi, O. M. *Chem. Rev.* **2014**, *114*, 1343. (c) Baerlocher, C.; McCusker, L. B. Database of Zeolite Structures, http://www.iza-structure.org/databases/.

(11) (a) Lohse, M. S.; Stassin, T.; Naudin, G.; Wuttke, S.; Ameloot, R.; De Vos, D.; Medina, D. D.; Bein, T. *Chem. Mater.* **2016**, *28*, 626. (b) Calik, M.; Sick, T.; Dogru, M.; Döblinger, M.; Datz, S.; Budde, H.; Hartschuh, A.; Auras, F.; Bein, T. *J. Am. Chem. Soc.* **2016**, *138*, 1234. (c) Bunck, D. N.; Dichtel, W. R. *Angew. Chem., Int. Ed.* **2012**, *51*, 1885.

(12) (a) Fischer, S.; Schmidt, J.; Strauch, P.; Thomas, A. *Angew. Chem., Int. Ed.* **2013**, *52*, 12174. (b) Fischer, S.; Schimanowitz, A.; Dawson, R.; Senkovska, I.; Kaskel, S.; Thomas, A. *J. Mater. Chem. A* **2014**, *2*, 11825. (c) Van Humbeck, J. F.; Aubrey, M. L.; Alsbaiee, A.; Ameloot, R.; Coates, G. W.; Dichtel, W. R.; Long, J. R. *Chem. Sci.* **2015**, *6*, 5499. (d) Chaoui, N.; Trunk, M.; Dawson, R.; Schmidt, J.; Thomas, A. *Chem. Soc. Rev.* **2017**, *46*, 3302.

(13) (a) Du, Y.; Yang, H.; Whiteley, J. M.; Wan, S.; Jin, Y.; Lee, S.-H.; Zhang, W. *Angew. Chem., Int. Ed.* **2016**, *55*, 1737. (b) Ma, H.; Liu, B.; Li, B.; Zhang, L.; Li, Y.-G.; Tan, H.-Q.; Zang, H.-Y.; Zhu, G. *J. Am. Chem. Soc.* **2016**, *138*, 5897. (c) Yu, S.-B.; Lyu, H.; Tian, J.; Wang, H.; Zhang, D.-W.; Liu, Y.; Li, Z.-T. *Polym. Chem.* **2016**, *7*, 3392. (d) Huang, N.; Wang, P.; Addicoat, M. A.; Heine, T.; Jiang, D. *Angew. Chem., Int. Ed.* **2017**, *56*, 4982. (e) Li, Z.; Li, H.; Guan, X.; Tang, J.; Yusran, Y.; Li, Z.; Xue, M.; Fang, Q.; Yan, Y.; Valtchev, V.; Qiu, S. *J. Am. Chem. Soc.* **2017**, *139*, 17771.

(14) O'Keeffe, M.; Peskov, M. A.; Ramsden, S. J.; Yaghi, O. M. *Acc. Chem. Res.* **2008**, *41*, 1782.

(15) Roeser, J.; Prill, D.; Bojdys, M. J.; Fayon, P.; Trewin, A.; Fitch, A. N.; Schmidt, M. U.; Thomas, A. *Nat. Chem.* **2017**, *9*, 977.

(16) Nguyen, N. T. T.; Furukawa, H.; Gándara, F.; Trickett, C. A.; Jeong, H. M.; Cordova, K. E.; Yaghi, O. M. *J. Am. Chem. Soc.* **2015**, *137*, 15394.

(17) Dogru, M.; Sonnauer, A.; Gavryushin, A.; Knochel, P.; Bein, T. *Chem. Commun.* **2011**, *47*, 1707.

(18) (a) Li, H.; Eddaoudi, M.; O'Keeffe, M.; Yaghi, O. M. *Nature* **1999**, *402*, 276. (b) Eddaoudi, M.; Kim, J.; O'Keeffe, M.; Yaghi, O. M. *J. Am. Chem. Soc.* **2002**, *124*, 376. (c) Rungtaweevoranit, B.; Diercks, C. S.; Kalmutzki, M. J.; Yaghi, O. *Faraday Discuss.* **2017**, *201*, 9.

(19) Zhao, Y.; Guo, L.; Gándara, F.; Ma, Y.; Liu, Z.; Zhu, C.; Lyu, H.; Trickett, C. A.; Kapustin, E. A.; Terasaki, O.; Yaghi, O. M. *J. Am. Chem. Soc.* **2017**, *139*, 13166.

(20) Hopper, S. P.; Tremelling, M. J.; Goldman, E. W. *J. Organomet. Chem.* **1980**, *191*, 363.

(21) Cella, J. A.; Cargioli, J. D.; Williams, E. A. *J. Organomet. Chem.* **1980**, *186*, 13.

DOI: 10.1021/jacs.8b01774
J. Am. Chem. Soc. 2018, 140, 5330−5333